International Journal of
Thermodynamics and Chemical Kinetics

ISSN 2456-6977
Volume 11, Issue 2, 2025
July–December
DOI (Journal): 10.37628/IJTCK

https://chemical.journalspub.info/index.php?journal=JTCK

Research IJTCK

Conceptual Design and Model Approach of an Amine Based on CO_2 Capture

Victor Chukwuemeka Ukpaka[1], Abraham Peter Ukpaka[2], Ukpaka, C. P.[3,*]

Abstract

The research works on the conceptual design and model approach of amine base CO_2 capture, Flue gases are conveyed through the absorber, where carbon dioxide is chemically absorbed using aqueous monoethanolamide (MEA) solution that is delivered to the column at its top. Due to the increased contact area between the phases, both phases travel through the packed bed where much of the chemical reaction takes place. Before entering the stripper, where the carbon dioxide is released with the aid of heat (resulting from the power plant cycle), the loaded (or rich) MEA solution (which contains absorbed CO_2) is preheated. From there, the solution is sent to the compression unit and transported to the storage location. After passing through the heat exchanger, which increases process efficiency, the recycled (lean) MEA enters the absorber prepared for the subsequent capture cycle. CO_2 is a greenhouse gas which contributes significantly to the rising temperatures of the planet. The conceptual approach and models needed to accomplish the goal and objectives of the CO_2 capture process for optimal performance are demonstrated in this study. The role of each part and the model equations to determine the equipment's capacity to carry out its function for absorbing CO_2 from the amine processing plant. The mass transfer and heat transfer are critical to the process plant's efficacy and efficiency. Therefore, the model equations and design importance are necessary.

Keywords: Conceptual, design, model, approach, amine, CO_2 capture, storage

INTRODUCTION

Greenhouse gas emissions are declining due to environmental concerns, especially the energy sector's significant reduction in carbon dioxide emissions. Carbon capture and storage (CCS) is thought to be the most efficient way to achieve CO_2 emission targets soon [1]. Among the different carbon capture and storage techniques, "post-combustion" capture – which includes absorption, adsorption, membrane, and cryogenic – is the most likely to be used in industry soon. Flue gases are passed through the absorber, which uses an aqueous monoethanolamine (MEA) solution that is supplied to the top of the column to chemically absorb carbon dioxide. Both phases pass through the packed bed where most of the chemical reaction occurs because of the larger contact area between them [2]. The loaded (or rich) MEA solution, which contains absorbed CO_2, is preheated before going into the strip, where the carbon dioxide is liberated with the help of heat (from the power plant cycle). The solution is then delivered to the storage area and sent to the compression unit. The recycled (lean) MEA enters the absorber ready for the next capture cycle after going via the heat exchanger, which improves process efficiency. Due to its high reactivity, affordability, and established behavior in other chemical sector installations, MEA is the most often used chemical solvent for CO_2 absorption [3].

***Author for Correspondence**
Ukpaka, C. P.
E-mail: peter.ukpaka@ust.edu.ng

[1]Research Student, College of Engineering, Computer Studies and Architecture, Department of Industrial Engineering, Lyceum of the Philippines University, Cavite, Philippines.
[2]Research Student, College of Engineering, Computer Studies and Architecture, Department of Computer Engineering, Lyceum of the Philippines University, Cavite, Philippines.
[3]Professor, Department of Chemical/Petrochemical Engineering, Rivers State University, Port Harcourt, Rivers State, Nigeria.

Received Date: February 27, 2025
Accepted Date: March 20, 2025
Published Date: March 25, 2025

Citation: Victor Chukwuemeka Ukpaka, Abraham Peter Ukpaka, Ukpaka C. P. Conceptual Design and Model Approach of an Amine Based on CO_2 Capture. International Journal of Thermodynamics and Chemical Kinetics. 2025; 11(2): 1–29p.

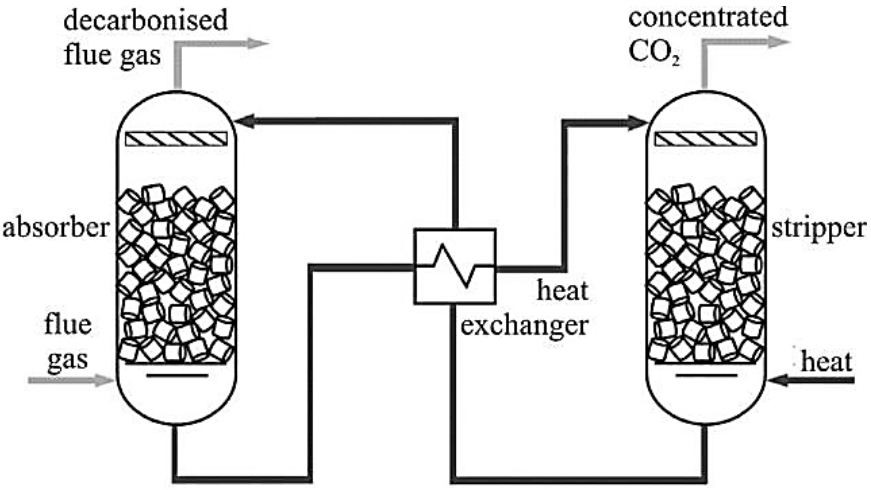

Figure 1. The process flow diagram for CO_2 absorption.

One greenhouse gas that has a major impact on the rising world temperatures is CO_2. Since the Industrial Revolution, the atmospheric CO_2 content has increased by 35% and is still rising significantly. If nothing is done in this area, the rate at which the CO_2 concentration is rising is unlikely to slow [4]. CO_2 concentration is the largest of all earth radiative components, contributing to a worldwide radiative forcing of 1.66 Wm^{-2}, according to the Intergovernmental Panel on Climate Change's (IPCC) Assessment Report. Fossil-fueled power plants, particularly those that use coal as their main fuel, are the main contributors of these emissions. Because CO_2 contributes to global warming, its reduction and absorption are there but the large flow rates of the flue gases with huge amount of CO_2 in it poses a serious challenge to such processes [5]. Post-combustion capture, oxyfuel combustion, and pre-combustion capture are the three main categories into which power plant CO_2 capture systems fall [6].

In post-combustion capture, CO_2 is extracted from the resulting flue gas after the fuel has burned. Figure 1 displays a schematic of the post-combustion capture. This approach requires a capture and compression mechanism illustrates how these technologies also necessitate that the flue gas be thoroughly cleaned prior to being fed into the collection equipment. Since sulfur dioxide and particulate matter cause corrosion and fouling, they must be eliminated. The main objective of this study is to develop an energy efficient absorption and capture system for CO_2 using monoethanolamine (MEA) solvent [7]. The objectives of these studies are to develop an effective flowsheet that accurately depicts the MEA-based CO_2 collecting and storage method [8]. The flowsheet needs to accurately depict the entire process, including all process machinery, finish the flowsheet by supplying accurate input data, chemical processes, and crucial design requirements needed for convergence and effective performance and research the impact of reboiler duty on factors, such as loading, capture %, temperature approach, and similar parameters, as well as to gather crucial data on operational limits and other working restrictions [9].

MATERIALS AND METHODS

Materials

The process flow diagram below illustrates the typical MEA scrubbing method of CO_2 capture. The absorber, the heat exchanger, and the stripper are the main components of the MEA process. The MEA solvent (Cold Lean MEA) and flue gas (Flue Gas) enter the absorber from the top and bottom, respectively. The MEA solvent selectively absorbs CO_2 with the use of an exothermic method. The CO_2-rich solvent (Cold Rich MEA) is discharged from the bottom of the absorber and passes through the heat exchanger to be preheated. Hot Rich MEA, a rich solvent that has been preheated, enters through the top hole of the stripper and desorbs CO_2 at high temperatures [10]. The stripper's bottom is drained by a CO_2-lean solvent (Hot Lean MEA), while the top collects CO_2. After the lean solvent has been chilled by going via the cooler and heat exchanger, the cold lean solvent (Cold Lean MEA) is recycled and enters the absorber's top [11–12].

List of Equipment

Absorber, heat exchanger and regenerator/stripper.

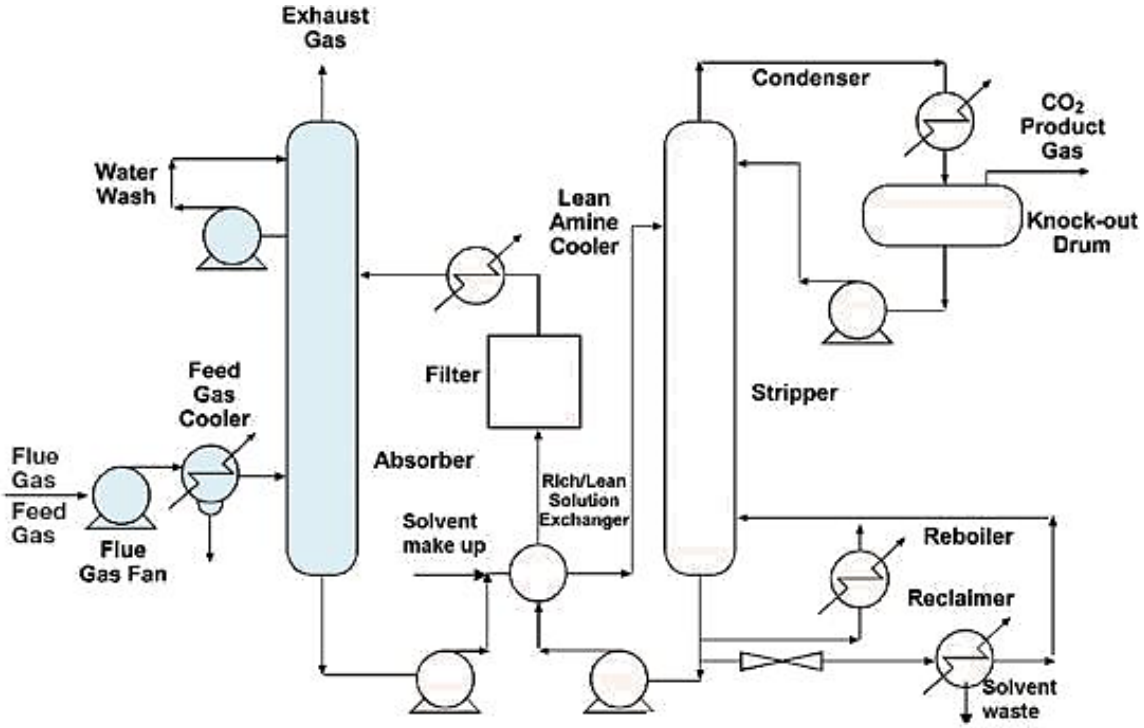

Figure 3. Process flow diagram for CO_2 capture.

METHODS

Parameters to Be Considered

The parameters listed below are supposed to be determined by an absorption column. The conditions of the gas and liquid streams entering and leaving the column, process variables, like pressure and temperature, the column's diameter, the column height, the column's pressure, decline and examine the composition of CO_2 gas using various solvents and the process flow diagram for CO_2 capture is presented in Figure 3.

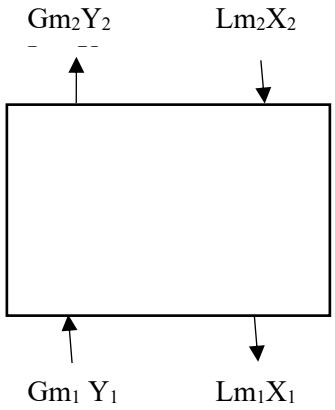

Figure 4. Schematic diagram of a packed bed absorption column undergoing countercurrent operation.

Material Balances in an Absorption Column

An absorption column facilitates gas–liquid contact, allowing a solute gas, such as CO_2, to be absorbed from a gas stream into a liquid. Within the column, the composition continuously changes from

one end to the other, as shown in Figure 4. Below are the fundamental material balance equations applicable to a counter-current absorption column.

Total Material Balance

Lm(2) + Gm(1) = Gm(2) + Lm(1)(1)L_m^{(2)} + G_m^{(1)}

= G_m^{(2)} + L_m^{(1)} \tag{1}Lm(2) + Gm(1) = Gm(2) + Lm(1) (1)

where

- Lm(1)L_m^{(1)}Lm(1): Liquid flow rate entering the column (bottom).
- Lm(2)L_m^{(2)}Lm(2): Liquid flow rate leaving the column (top).
- Gm(1)G_m^{(1)}Gm(1): Gas flow rate entering the column (bottom).
- Gm(2)G_m^{(2)}Gm(2): Gas flow rate leaving the column (top).

CO_2 Component Material Balance

Lm(2)X2 + Gm(1)Y1 = Gm(2)Y2 + Lm(1)X1(2)L_m^{(2)} X_2 + G_m^{(1)} Y_1

= G_m^{(2)} Y_2 + L_m^{(1)} X_1 \tag{2}Lm(2)X2 + Gm(1)Y1

= Gm(2)Y2 + Lm(1)X1 (2)

where

- X1X_1X1: Mole fraction of CO_2 in the liquid entering (bottom).
- X2X_2X2: Mole fraction of CO_2 in the liquid leaving (top).
- Y1Y_1Y1: Mole fraction of CO_2 in the gas entering (bottom).
- Y2Y_2Y2: Mole fraction of CO_2 in the gas leaving (top).

CO_2 Balance (Assuming Equimolar Counter-Current Flow Rates)

If the gas and liquid flow rates are equimolar,

Gm(Y1 − Y2) = Lm(X1 − X2)(3)G_m (Y_1 – Y_2)

= L_m (X_1 – X_2) \tag{3}Gm (Y1 −Y2)

= Lm (X1 −X2) (3)

Operating Line Equation

The operating line represents the relationship between liquid and gas compositions across the column.

Y = LmGmX + Y2 − LmGmX2(4)Y

= \frac{L_m}{G_m} X + Y_2 – \frac{L_m}{G_m} X_2 \tag{4}Y

= GmLmX + Y2 − GmLmX2 (4)

In case the liquid entering is CO_2-free, i.e., X2 = 0X_2 = 0X2=0,

Y = LmGmX + Y2(5)Y = \frac{L_m}{G_m} X + Y_2 \tag{5}Y = GmLmX + Y2 (5)

Determining Stream Rates

In a packed absorption column operating at dilute concentrations and equimolar counter-current flow:

- *Gas Flow Rate:*

Gm = Gm(1) = Gm(2)(6)G_m = G_m^{(1)} = G_m^{(2)} \tag{6}Gm = Gm(1) = Gm(2) (6)

- *If entering solvent is free of CO_2*, i.e., X2 = 0X_2 = 0X2 = 0, and Y2Y_2Y2 is the CO_2 concentration in exit gas:

$$Gm = LmX1Y1 - Y2(7)G_m = \frac{L_m X_1}{Y_1 - Y_2} \tag{7}Gm = Y1 - Y2LmX1$$

- *Liquid-to-Gas Ratio:*

$$LmGm = Y1 - Y2X1 - X2(8)\frac{L_m}{G_m} = \frac{Y_1 - Y_2}{X_1 - X_2} \tag{8}GmLm = X1-X2Y1-Y2$$

- *For dilute systems with X2=0X_2 = 0X2=0:*

$$X1 = GmLm(Y1 - Y2)(9)X_1 = \frac{G_m}{L_m} (Y_1 - Y_2) \tag{9}X1 = LmGm(Y1 - Y2)$$

Selection of Packing

Packing materials provide surface area for gas–liquid contact. There are four major classifications,

1. Broken Solids.
2. Shaped Packings.
3. Grids.
4. Structured Packings.

In this design, the following types of packaging are considered,

- Intalox Saddle.
- Pall Rings.
- Ceramic Intalox Saddle.

Standard packing properties include,

- *Size:* 10 mm to 100 mm.
- *Surface Area:* Varies by type.
- *Packing Factor:* Important for pressure drop and efficiency.

Note: The ceramic Intalox saddle is considered twice for emphasis due to its high performance in corrosion resistance and thermal stability [12–16].

Determination of Column Diameter

The column diameter is a crucial factor in the design of absorption columns. It is influenced by the volumes of gas and liquid handled, their characteristics, and the ratio of one stream to another.

To determine the surface area,

$$A_c = \frac{Gm}{V_w} \tag{11}$$

A_c = Area of the column, Gm = Gas flow rate, V_w = gas mass flow rate per unit column cross sectional area in kg/m^{2}S.

To determine V_w,

$$K_4 = \frac{13.13(V_w)^2 F_p \left(\frac{\mu_l}{\rho l}\right)^{0.1}}{\rho_v(\rho_l - \rho_v)} \tag{12}$$

$$V_w = \left[\frac{K_4 \rho_v (\rho_l - \rho_v)}{13.13\left(\frac{\mu_l}{\rho l}\right)^{0.1}}\right]^{\frac{1}{2}} \quad (13)$$

F_p = packing factor in m^{-1}, μ_l = liquid velocity in Ns/m^2, ρ_l, ρ_v= liquid and vapor densities in kg/m^3

The value of K_4 is gotten from the graph correlation of K_4 with liquid vapour flow factor (F_{LV}) can be determined by using the information from the chart in Figure 5.

$$F_{LV} = \frac{ln}{Vn}\sqrt{\frac{\rho_v}{\rho_l}}$$

Hence, to determine the diameter of the column,

$$D_c = \sqrt{\frac{4A_c}{\pi}} \quad (14)$$

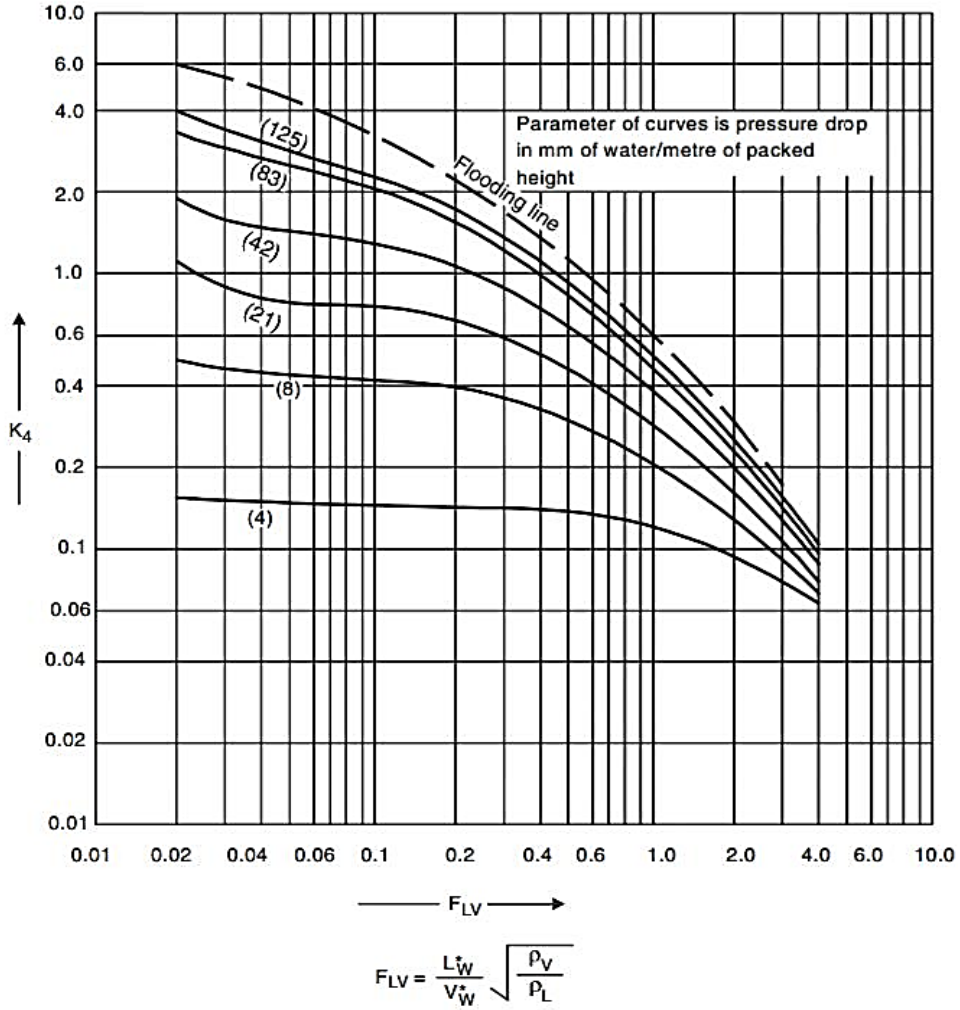

Figure 5. Generalized pressure drop correlation for K_4.

Height of the Column and Height Equivalent of a Packing (HETP)

The degree of concentration fluctuations and the rate of mass transfer per unit of the packed column determine the height of the column and, consequently, the total volume of packing.

$$Z = H_{OG}N_{OG} \tag{15}$$

H_{OG} is the height of the overall gas phase transfer unit and N_{OG} is the number of overall gas phase transfer unit.

To calculatethe value of N_{OG},

$$N_{OG}=\int_{Y_2}^{Y_1}\frac{dy}{y-ye} \tag{16}$$

It can also be expressed in terms of pressure.

$$N_{OG} = \int_{Y_2}^{Y_1}\frac{dy}{y-ye} \tag{17}$$

To calculate the value of H_{OG}

$$H_{OG}=\frac{G_m}{K_G aP} \tag{18}$$

Therefore,

$$Z = \frac{G_m}{K_G aP}\int_{Y_2}^{Y_1}\frac{dy}{y-ye} \tag{19}$$

Z = height of the column in m, G_m = gas flow rate per unit cross sectional area, Y_1 = mole fraction of CO_2 entering the column from bottom, Y_2 = mole fraction of CO_2 at the top of the column, Y_e = concentration in the gas that would be in equilibrium with the liquid concentration, P = total pressure, a = interfacial surface area per unit volume and K_G= the overall gas phase mass transfer coefficients. The relationship between equilibrium concentration and actual concentration is shown below in Figure 6.

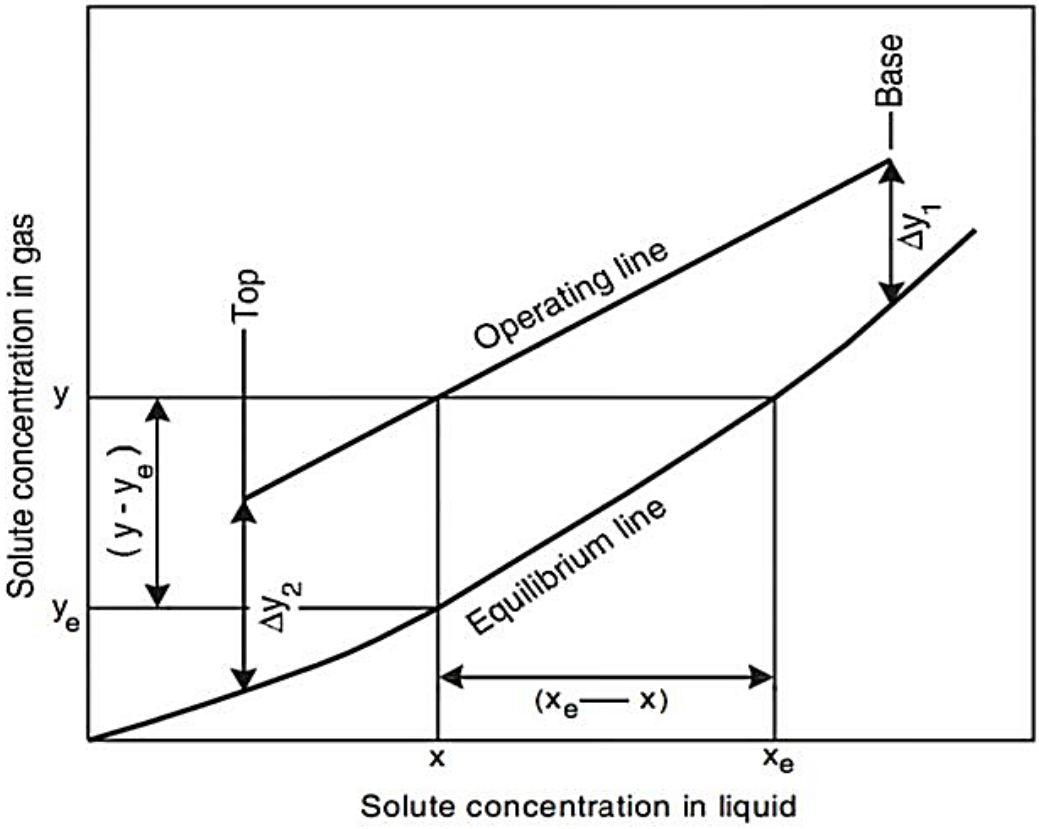

Figure 6. Gas absorption concentration relationship.

Height Equivalent of Packing (HETP)

In packed columns, the HETP is defined as the height of the packed column necessary to give a separation equal to one theoretical stage, it can be calculated using H_{OG} value.

$$HETP = \frac{\left[H_{OG} ln\left(\frac{mG_m}{L_m}\right)\right]}{\left[\frac{mG_m}{L_m} - 1\right]} \tag{20}$$

The graph of calculating N_{OG} is given below using the slope and mole fractions that are shown in Figure 7.

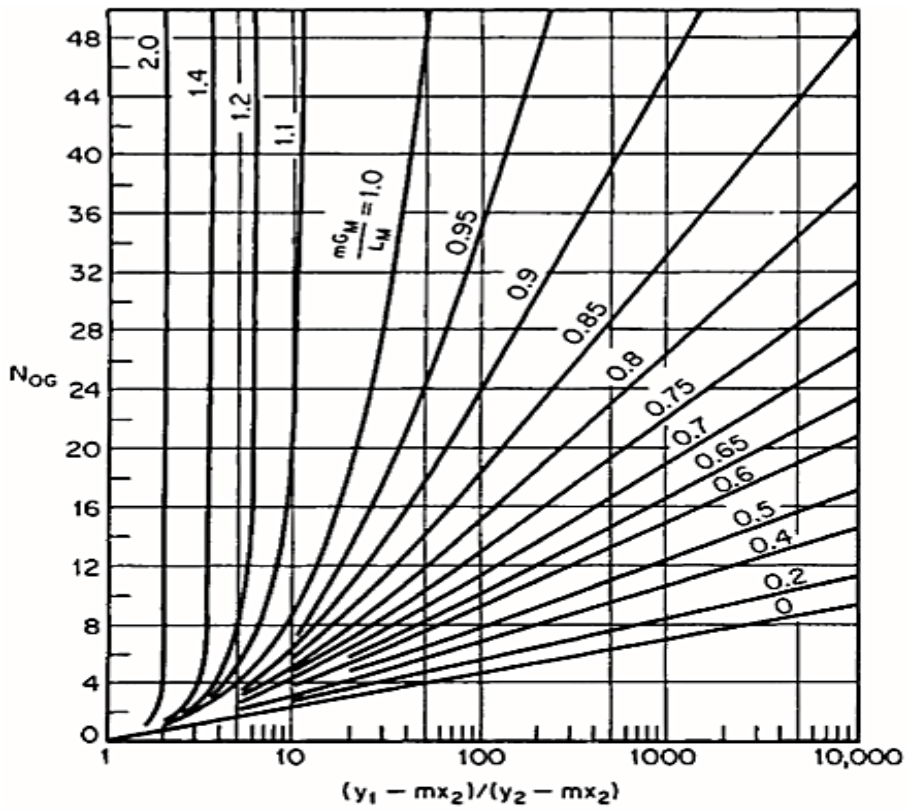

Figure 7. Number of overall gas phase mass transfer units in a packed column.

Efficiency of an Absorption Column

To estimate the overall efficiency of a packed column, the equation below can be used using O' Connell relation.

$$E_0 = 1.97 - 0.199\left(\frac{mM_l\mu_l}{\rho_l}\right) - 0.00896\left[log\left(\frac{mM_l\mu_l}{\rho_l}\right)\right]^2$$

E_0 is average % efficiency, M_l is Molecular weight of the liquid, m is the slope of the equilibrium line in mole fraction units, ρ_l is the liquid density.

μ_l is the molar average liquid viscosity in cp at the average column temperature.

Flows in Packed Columns

Pressure Drops

It is crucial to be able to anticipate the pressure reduction as the two fluid streams pass through a densely packed column.

$$-dPw = -dP_d\left(1 + \frac{3.30}{dn}\right) \tag{21}$$

$-dP_w$ is the pressure drop across the wet drained column, $-dP_d$ is the pressure drop across the dry column, and dn is the nominal size of the Rasching rings in mm.

The work of Morris and Jackson, who compiled experimental data for a variety of ring and grid packings in a graphical format useful for calculating the number of velocity heads N lost per unit height of packing, represents a different strategy. In the equation, N is substituted,

$$-dP = \frac{1}{2} N \rho_G U^2_G l \tag{22}$$

where $-dP$ = pressure drop measured in N/m^2, ρ_G = gas density in kg/m, N = number of velocity heads N lost per unit height of packing in m^{-1}, U_G = gas velocity, in m/s, l = height of packing measured in m.

Loading and Flooding Points

Sherwood et al.'s graph relation can be used to determine the flooding point of a packed column.

$U_{G^2} \frac{S_B}{[3]} \left(\frac{\rho_G}{\rho_L}\right) \left(\frac{\mu_G}{\mu_L}\right)^{0.2}$ is plotted against $\frac{L'}{G'} \sqrt{\left(\frac{\rho_G}{\rho_L}\right)}$

U_G= velocity of gas, S_B = surface area of the packing per unit volume of the bed, g = acceleration due to gravity, L' = mass rate of the flow per unit area of the liquid, G' = the mass rate of flow per unit area of the gas, μ_G/μ_L= viscosity of gas and liquid

$\frac{\rho_G}{\rho_L}$ = density of gas and liquid

The area inside the curve represents possible conditions of operation of Figure 8.

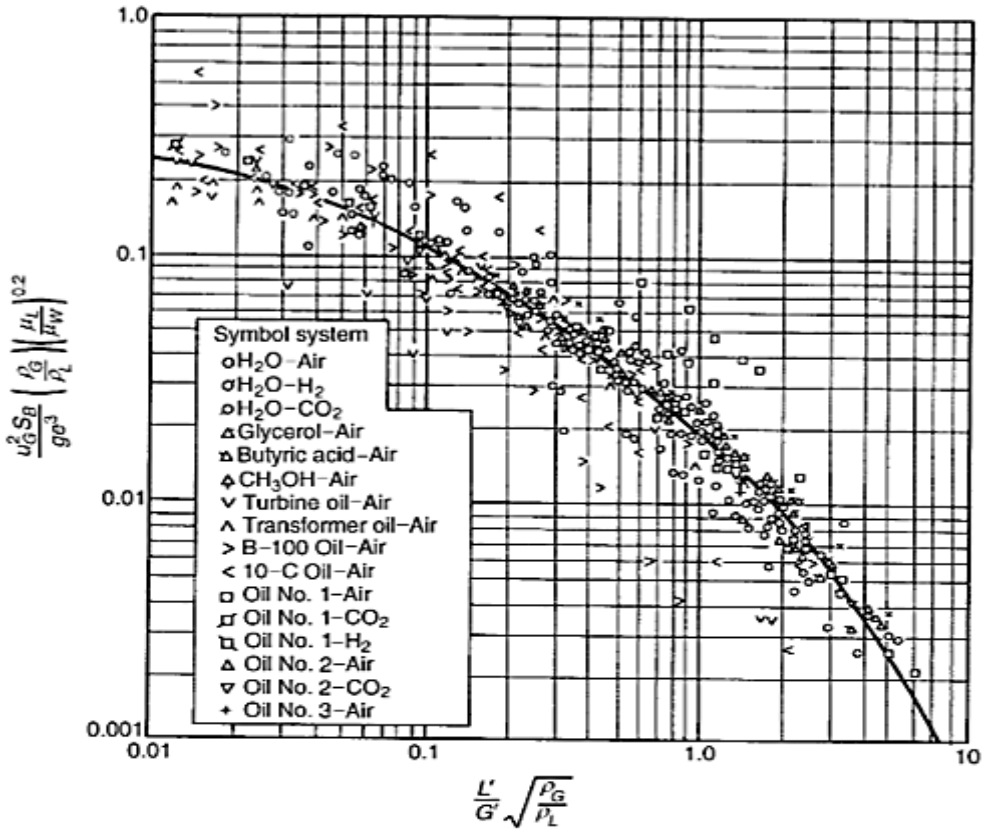

Figure 8. Chart of flooding calculation [4].

Liquid Distribution

Unless the liquid is spread evenly over the packing's surface, a packing with a high surface area per unit volume may not produce good gas and liquid contacting. This suggests that the liquid should be dispersed evenly across the packing's surface.

$$L_w = \frac{V}{A} \tag{23}$$

L_w = wetting rate, V= volumetric liquid rate per unit cross-sectional area of column, A= packing surface area per unit volume of column. It is also calculated as,

$$L_w = \frac{L}{A\rho_L S_B} = \frac{\mu_L}{S_B} \tag{24}$$

S_B = the surface area of the packing per unit volume of the bed, L_w= wetting rate and ρ_L = density of the liquid

A = Area

Therefore, the wetting rate is analogous to the volumetric liquid rate per unit length.

Design of the Distillation Column

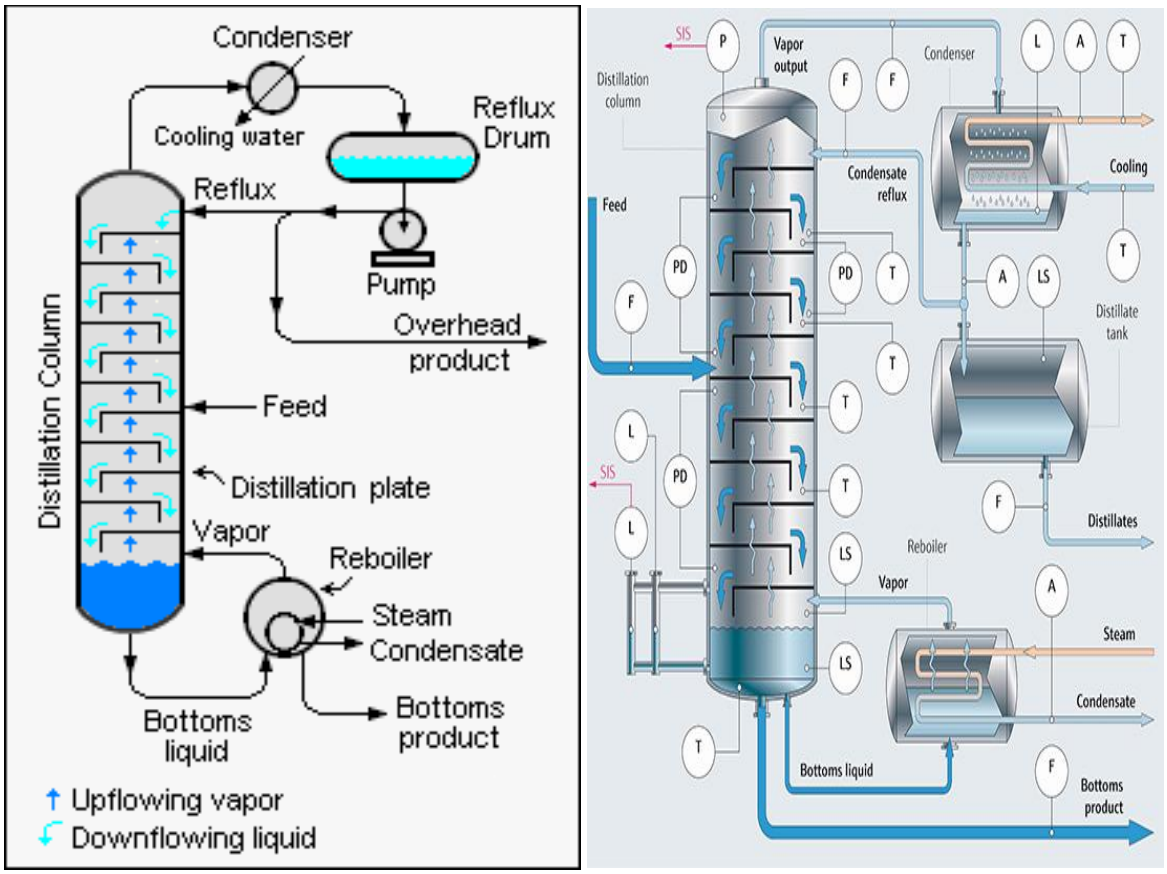

Figure 9. Distillation column: (a) basic column, (b) multiple feed.

The steps in the design of a distillation column are as follows, which is illustrated in Figure 9.

1) Specify the level of isolation necessary to establish product requirements.
2) Decide whether the operation will be batch or continuous, and the operating pressure.

3) Decide whether to use plates or packing as the contacting device.
4) Calculate the number of equilibrium stages and the stage and reflux requirements.
5) The column's size, i.e., diameter and actual stage count.
6) Design the plates, distributors, and packing supports for the column's interior.
7) Mechanical design, i.e., internal fixtures and the vessel.

Identifying the stage and reflux requirements will be the first step. When the feed is a binary mixture, this technique is rather straightforward. However, when the feed has more than two components, it becomes a complex and challenging task.

Definition of Terms Around the Distillation Column

Reflux Considerations

The reflux ratio, R, is normally defined as:

$$R = \frac{L_n}{D} = \frac{flowreturnedasreflux}{flowgoingoutatthetop(distillate)} \tag{25}$$

Depending on the reflux ratio applied, the number of stages needed for a particular separation will vary. In a functioning column, vapor condensation caused by heat loss via the walls will raise the effective reflux ratio. The heat loss from a well-lagged column will be minimal, therefore, design calculations often do not take this enhanced flow into account. If a column has inadequate insulation, changes in internal reflux brought on by abrupt changes in the environment, like a sudden downpour, can significantly affect the column's performance and control.

Types of Refluxes

There are different types of refluxes with their own unique properties; total reflux, minimum reflux and optimum reflux ratio.

Total Reflux

Total reflux occurs when no product is removed from the condensate and no feed is provided, causing it to return to the column as reflux. The lowest at which it is theoretically possible to achieve the separation is at total reflux, which corresponds to the number of steps needed for a specific separation. Although not actual operational conditions, it serves as a helpful indicator of how many steps are likely to be required. It is common practice to start up columns without any product take-off and run them at total reflux until stable conditions are reached. It is also practical to test columns while they are completely refluxed.

Minimum Reflux

A pinch point where the separation can only be accomplished with an endless number of stages will appear as the reflux ratio is reduced. For the specified separation, this establishes the lowest feasible reflux ratio.

Optimum Reflux Ratio

Between the minimum for the stated separation and total reflux, practical reflux ratios will fall. The designer must decide on a value at which the required separation is attained for the lowest possible price. Reducing the number of necessary stages and, thus, the capital cost by increasing reflux increases operational expenses and service requirements (steam and water). The reflux ratio that results in the lowest yearly operating cost is the one that should be used. Although there are no hard and fast guidelines for choosing the design reflux ratio, for many systems the ideal will be between 1.2 and 1.5 times the minimum reflux ratio. The short-cut design approaches presented in this chapter can be used to study the effect of reflux ratio on the number of stages for new designs where the ratio cannot be

determined from previous experience. This will typically highlight the optimum value to apply to stricter design methodologies.

The calculated number of steps for low reflux ratios will be greatly influenced by the precision of the given vapor–liquid equilibrium data. A larger than normal ratio should be chosen to increase trust in the design if the data are doubtful.

Feed Point Location

The precise location of the feed point will affect the number of stages required for a specified separation and the subsequent operation of the column. As a rule, the feed should enter the column at the point that gives the best match between the feed composition (vapor and liquid if two phases) and the vapor and liquid streams in the column. In practice, it is wise to provide two or three feed-point nozzles located round the predicted feed point to allow for uncertainties in the design calculations and data, and possible changes in the feed composition after start-up.

Selection of Column Pressure

The key factor in choosing the column operating pressure will be to make sure the distillate's dew point is higher than what can be conveniently obtained with the plant cooling water, unless you are distilling heat-sensitive compounds. The standard for the maximum summer cooling water temperature is 30ºC. The provision of refrigerated brine cooling should be taken into consideration if this means that high pressures will be required. Where very high temperatures would ordinarily be required to distill comparatively non-volatile compounds, vacuum operation is employed to lower the column temperatures for the distillation of heat-sensitive materials. It is customary to assume that the operating pressure remains constant throughout the column when computing the stage and reflux requirements. When determining the stage temperatures, it is important to account for the fact that the column pressure decrease in vacuum columns will represent a sizeable portion of the overall pressure. As it is obvious that the pressure drop cannot be determined before an estimate of the number of stages is made, this may need a trial-and-error computation.

Equations Involved in the Design of a Distillation Column

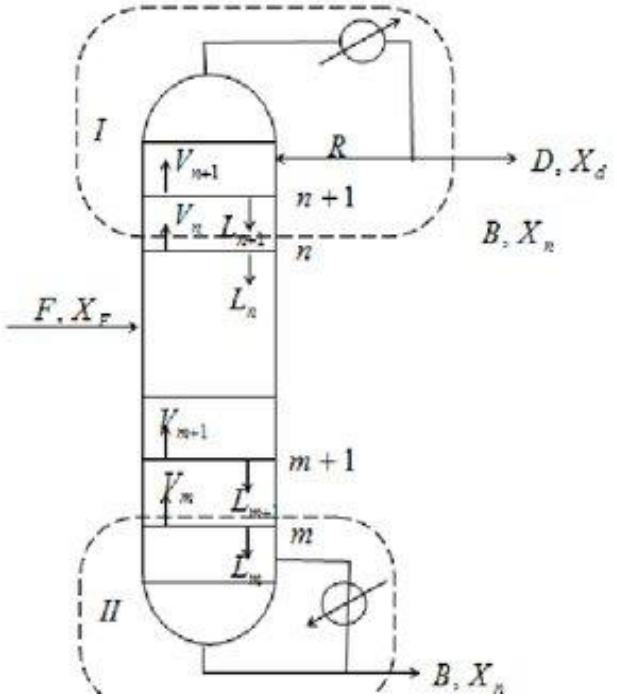

Figure 10. Column flow and composition above and below feed [4].

The fundamental stage equations were created and used for the study of binary systems. The top of a column's flows and compositions are depicted in Figure 10. The following equations result from expanding the system boundary to include stage "n" and the condenser.

Taking Material Balance

The top section around the condenser is the rectifying column while the bottom section around the reboiler is the stripping section. Let "c" denote CO_2 going into the feed and coming out as both top and bottom product.

∴ Taking material balance on the rectifying section,

Input = Output

$$V_n = L_{n+1} + D \tag{26}$$

Taking component balance on the rectifying section,

$$V_n y_n = L_{n+1} x_{n+1} + D x_{d,c} \tag{27}$$

∴ Taking energy balance on the rectifying section.

In energy balance we consider both enthalpy and heat.

Input = Output

$$V_n H_n = L_{n+1} h_{n+1} + D h_{d,c} + q_{c,c}$$

where $q_{c,c}$ is the heat removed in the condenser.

From the Equations above (26) and (27),

$$V_n y_n = L_n x_{n+1} + D x_{d,c} \tag{26}$$

$$y_n = \frac{L_n}{V_n} x_{n+1} + \frac{D}{V_n} x_{d,c} \tag{27}$$

But $V_n = L_{n+1} + D$

$$\therefore y_n = \frac{L_n}{L_{n+1}+D} x_{n+1} + \frac{D}{L_{n+1}+D} x_{d,c} \tag{28}$$

Divide both numerator and denominator by D,

$$\therefore y_n = \frac{\frac{L_n}{D}}{\frac{L_{n+1}}{D}+\frac{D}{D}} x_{n+1} + \frac{\frac{D}{D}}{\frac{L_{n+1}}{D}+\frac{D}{D}} x_{d,c} \tag{29}$$

Recall reflux; $R = \frac{L_n}{D} = \frac{L_{n+1}}{D}$

$$\therefore y_n = \frac{R}{R+1} x_{n+1} + \frac{1}{R+1} x_{d,c} \tag{30}$$

Taking material balance on the bottom section (stripping section),

$$V_m = L_{m+1} + B \tag{31}$$

Taking component balance on the bottom section,

$$V_m y_m = L_{m+1} x_{m+1} + B x_{b,c} \tag{32}$$

Energy balance on the bottom section,

$$V_m H_m = L_{m+1} h_{m+1} + B h_{b,c} - q_{b,c} \tag{33}$$

From Equation (32),

$$y_m = \frac{L_{m+1}}{V_m} x_{m+1} + \frac{B}{V_m} x_{b,c} \tag{34}$$

where, $q_{b,c} = heatadded \in thereboiler$

Material balance around the feed (feed section),

$$L_m = L_n + qF \tag{35}$$

where

$$q = heatvapouriseonemoloffeed \frac{}{molarlatentheatoffeed} = \frac{m\lambda + m(H_{fs} - H_f)}{m\lambda} \tag{36}$$

$$\therefore q = \frac{\lambda + (H_{fs} - H_f)}{\lambda} \tag{36a}$$

Composition balance.

$$y_q = \frac{L_m}{V_m} x_q + \frac{B}{V_m} x_m \tag{37}$$

The value of q depends on the nature of feed.

Q-line and feed conditions are presented in Figure 11.

Types,

a. Sub cooled feed (q1).
b. Saturated liquid ($q = 1$).
c. Superheated vapor ($q < 1$).
d. Saturated vapor ($q = 0$).
e. Partially vaporized feed ($0 < q < 1$).

Lewis–Sorel Method (Equimolar Overflow)

Lewis originally suggested a simplifying assumption for most distillation problems, which negates the necessity to solve the stage energy-balance equations. The stripping and rectifying parts assume a constant molar liquid and vapor flow rate. Equimolar overflow is the state in which the molar liquid and vapor flows from each stage are constant. This will only be the case if there is no significant heat mixing, the component molar latent heats of vaporization are identical, and the specific heats are constant over the temperature range in the column. When the constituents combine to generate nearly perfect liquid mixtures, these conditions are essentially true for real-world systems.

$$y_n = \frac{L}{L+D} x_n + \frac{D}{L+D} x_{d,c} \tag{40}$$

Also,

$$x_n = \frac{V'}{V'+B} y_n + \frac{B}{V'+B} x_{b,c} \tag{41}$$

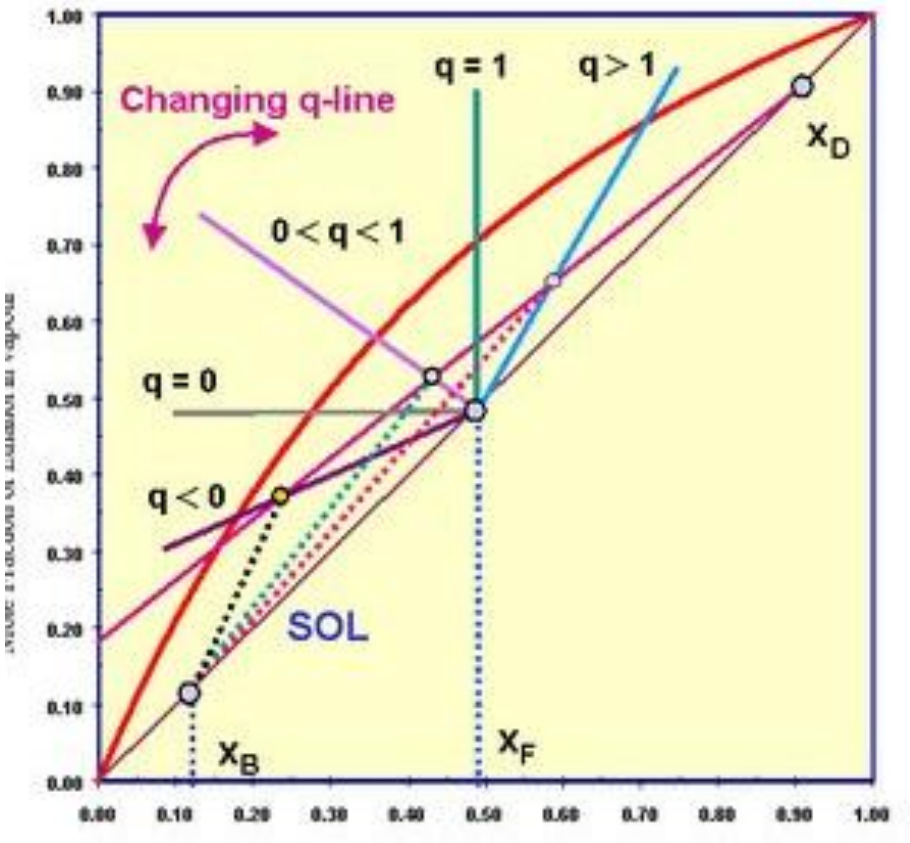

Figure 11. Different types of q-line.

where L is the constant liquid flow in the rectifying section.

Equations (40) and (41) can also be in the form,

$$y_n = \frac{L}{V}x_n + \frac{D}{V}x_{d,c} \tag{42}$$

$$y_m = \frac{L'}{V'}x_{n+1} + \frac{B}{V'}x_{b,c} \tag{43}$$

where, V is the constant vapor flow in the rectifying section = L+ D and L' is the constant liquid flow in the stripping section = $V' + B$

Determination of Number of Plates in a Distillation Column

Equations (42) and (43) and the equilibrium relationship are conveniently solved by the graphical method developed [10]. The method is discussed fully in Volume 2, Coulson and Richardson.

Steps Involved in Constructing McCabe–Thiele Diagram

In reference to Figure 12, all compositions are those of the more volatile component.

All compositions in Figure 12 are those of the more volatile component.

1. Using the information provided at the column operating pressure, plot the vapor–liquid equilibrium curve. Using equal scales for the x- and y-axis is typically more practical and less confusing. In terms of relative volatility, where is the geometric average relative volatility of the lighter (more volatile) component with respect to the heavier component (less volatile).

$$y = \frac{\alpha x}{(1+(\alpha-1)x)} \tag{44}$$

2. To calculate the top and bottom compositions, $x_{d,c}$ and $x_{b,c}$, from the above data, do a material balancing over the column.
3. Mark the locations on the diagram where the top and bottom operating lines, respectively, intersect the diagonal at $x_{d,c}$ and $x_{b.c}$.
4. The phase state of the feed determines where the two operational lines will intersect. The q line is the line on which the intersection occurs.

The Q-line is found as,

Calculate the value of the ratio q given by Equations (36) and (36a),

$$q = heatvapouriseonemoloffeed\frac{}{molarlatentheatoffeed} = \frac{m\lambda + m(H_{fs} - H_f)}{m\lambda}$$

1. Plot the q line, slope $q/(q-1)$, intersecting the diagonal at $x_{f,c}$ (the feed composition).
2. Select the reflux ratio and determine the point where the top operating line extended cuts the y axis:

$$\emptyset = \frac{x_d}{1+R}$$

3. Draw in the top operating line, from $x_{d,c}$ on the diagonal.
4. Draw in the bottom operating line from $x_{b,c}$ on the diagonal to the point of intersection of the top operating line and the q line.
5. Starting at $x_{d,c}$ or $x_{b,c}$, step off the number of stages.

Note: On the stage nearest to the point where the operational lines converge, place the feed point. The partial condenser, if employed, and the reboiler serve as equilibrium stages. To account for this while designing a column, however, would be counterproductive because these could be viewed as extra safety features.

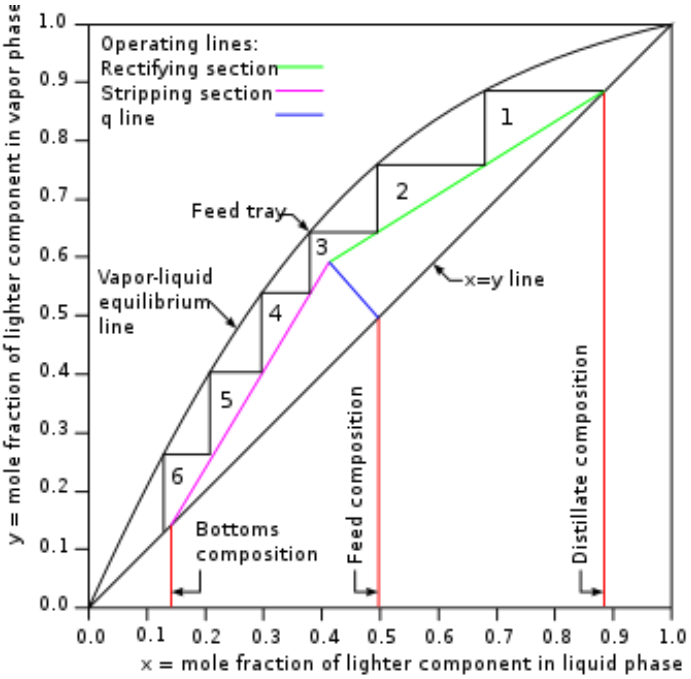

Figure 12. McCabe–Thiele plot [4].

Other Types of Distillation Column System

Batch Distillation

The still typically consists of a vessel with a plate or packed column atop it. Either the heater is built into the vessel, or a separate reboiler is employed. The following situations warrant considering batch distillation: When there is a minimal amount of material to distill, an environment where a variety of goods must be manufactured, a location where the feed is sporadically produced and in cases where the content of the feed varies greatly.

As the batch is distilled, the composition in the still's bottoms changes, making batch distillation an unstable state process. There are two operating modes.

1. Fixed reflux, where the reflux rate is fixed. The distillation is stopped when the average composition of the collected distillate, or the remaining bottoms, satisfies the necessary requirements. As the more volatile component is distilled off, the compositions will alter.
2. Variable reflux, which modifies the reflux rate during the distillation process to produce a fixed overhead composition. It will be necessary to progressively increase the reflux ratio as the percentage of the more volatile component in the still's base falls.

Steam Distillation

It is used to distill substances with high boiling points and goods that are sensitive to heat. Vacuum distillation can be substituted by this method. Water must be soluble in the products. Normally, some steam will be permitted to condense to supply the heat needed for the distillation. Live steam, as well as steam produced by a heater in the still or in an external boiler, can be immediately pumped into the base of the column.

Reactive Distillation

The following benefits result from carrying out the reaction with product separation and distillation.

1. Restrictions on chemical equilibrium are removed because the product is eliminated as it is created.
2. Energy savings are possible since distillation can use the reaction heat.
3. Since only one vessel is needed, capital expenses are decreased.

Sundmacher and Kiene provide a thorough explanation of the procedure.

Plate-Design Procedure

To create a successful design, a trial-and-error process is required. Starting with a crude plate layout, critical performance criteria must be checked, and the design must be revised as needed. The steps of a typical design process are outlined below and covered in the sections that follow. The discussion includes the typical range for each design variable as well as suggested numbers that can be utilized to kick off the design.

Procedures

Calculate the column diameter using flooding factors, choose the liquid flow configuration, layout a trial plate with the following elements: downcomer area, active area, hole area, hole size, and weir height, check the weeping rate; if it is too high, go back to step 6, verify the plate pressure drop; if it is excessive, go back to step 6, if the back-up from the downcomer is too high, go back to step 6 or 3, choose the specifics of the plate arrangement, such as the soothing zones and the unperforated portions. If the hole pitch is not satisfactory, go back to step 6, recalculate the flooding percentage using the selected column diameter, verify entrainment.

Plate Area

The following areas terms are used in the plate design procedure: $A_c =$ total column cross-sectional area and $A_d =$ cross-sectional area of downcomer, $A_n =$ net area available for vapor-liquid disengagement, normally equal to $A_c - A_d$ for a single pass plate, A_a= active, or bubbling, area, equal to $A_c - 2A_d$ for single-pass plates, A_h = hole area, the total area of all the active holes, A_p = perforated area (including blanked areas) and A_{ap} = the clearance area under the downcomer apron.

Column Diameter

The flooding state determines the top limit of the vapor velocity. A high vapor velocity, usually between 70% and 90% of what would cause flooding, is necessary for high plate efficiencies. When calculating the diameter, the area of the column should be between 80% and 85% of the flooding velocity. The column area is also obtained by dividing the maximum volumetric vapor flow rate (m^3/s) by the actual vapor velocity (m/s) considered for the design, where the corresponding multipliers are 1.0, 0.9, and 0.8, and the hole active areas are 0.10, 0.07, and 0.06.

$$A_c = \frac{maximumvolumetricvapourflowrate(m^3/s)}{actualvapourvelocity(m/s)} \tag{46}$$

So that, diameter of column D_c,

$$D_c = \sqrt{\frac{A_c \times 4}{\pi}} \tag{47}$$

The Fair (1961) correlation can be used to determine the flooding velocity.

$$u_f = k_1 \sqrt{\frac{\rho_{L-\rho_V}}{\rho_V}} \tag{48}$$

where, u_f = flooding vapour velocity, m/s, based on the net column cross-sectional area A_n,
k_1 = a constant obtained from the figure below (Figure 13).

The following restrictions apply to the use of Figure 13.

1. Hole size less than 6.5 mm. Entrainment may be greater with larger hole sizes.
2. Weir height is less than 15 percent of the plate spacing.
3. Non-foaming systems.
4. *Hole:* active area ratio greater than 0.10; for other ratios apply the following corrections.
5. Liquid surface tension 0.02 N/m, for other surface tensions multiply the value of K_1 by $(\sigma/0.02)^{0.2}$.
6. The liquid vapor flow factor F_{LV} in Figure 13 is given by,

$$F_{LV} = \frac{L_w}{V_w}\sqrt{\frac{\rho_V}{\rho_L}} \tag{49}$$

where, L_w is the liquid mass flow rate, kg/s.
V_w is the vapour mass flow rate, kg/s.

7. To calculate the column diameter an estimate of the net area A_n is required. As a first trial, take the downcomer area as 12 percent of the total, and assume that the hole active area is 10 percent.
8. Where the vapor and liquid flowrates, or physical properties, vary significantly throughout the column, a plate design should be made for several points up the column. For distillation it will usually be sufficient to design for the conditions above and below the feed points. Changes in the vapor flowrate will normally be accommodated by adjusting the whole area; often by blanking off some rows of holes. Different column diameters would only be used where there is a considerable change in flowrate. Changes in liquid rate can be allowed by adjusting the liquid downcomer areas.

Liquid Flow Arrangement

Reverse, single pass, or multiple pass plates can be used, depending on the liquid flow rate and column diameter. Figure 14 which was modified from a similar illustration provided, can be used to make a first choice.

Entrainment

Entrainment can be estimated from the correlation given in Figure 15 which gives the fractional entrainment ψ (kg/kg gross liquid flow) as a function of the liquid–vapor factor F_{LV}, with the percentage approach to flooding as a parameter. The percentage flooding is given by,

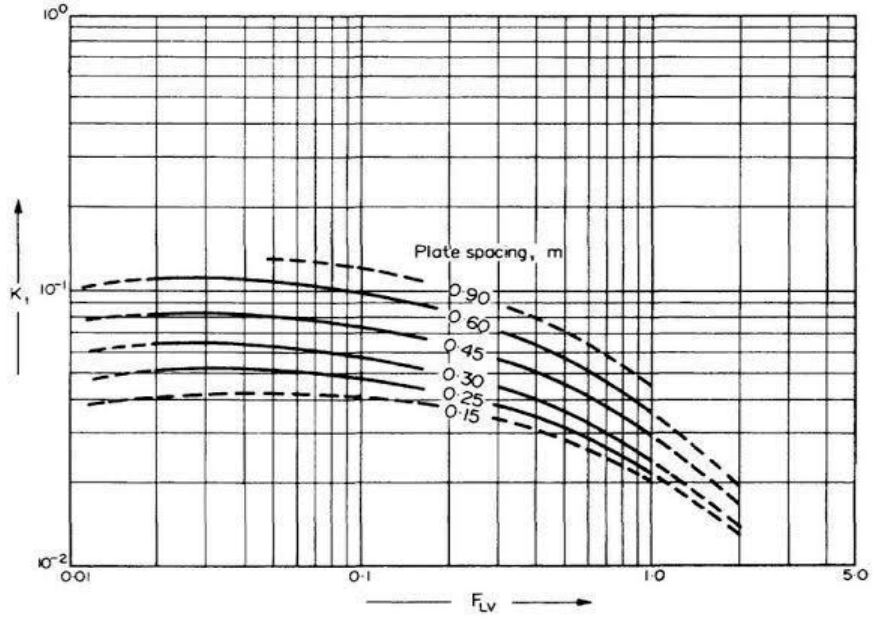

Figure 13. Flooding velocity sieve plate [4].

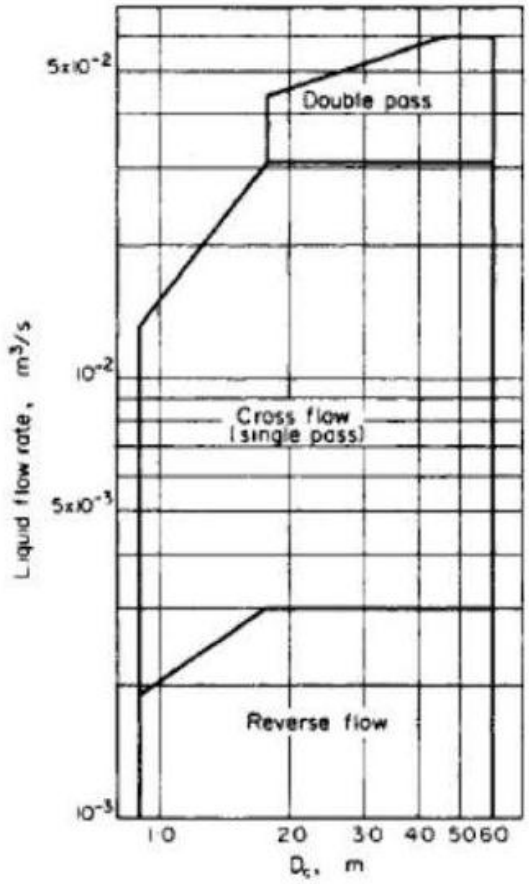

Figure 14. Selection of liquid flow arrangement [4].

$$Percentageflooding = \frac{U_n}{U_f} = \frac{actualvelocity(basedonnetarea)}{equation3.48} \quad (50)$$

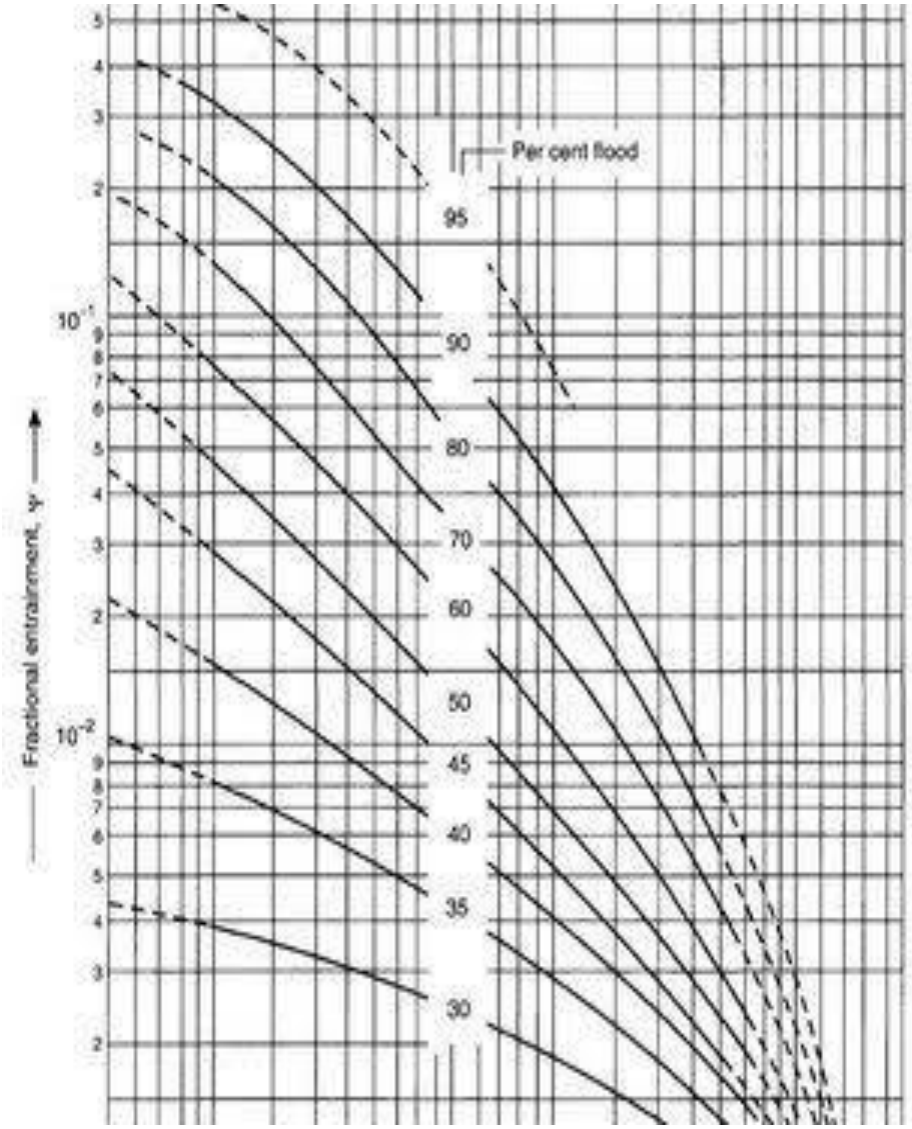

Figure 15. Entrainment correlations of sieve plates [4].

Weep Point

The lower limit of the working range is achieved when large volumes of liquid seep through the plate perforations. This is the weep point. The vapor velocity at the weep point is the lowest value required for stable operation. Even at the lowest running rate, the entire region must be chosen so that the vapor flow velocity remains significantly higher than the weep points. For details on several correlations proposed to predict the vapor velocity at the weep point. As seen in Figure 16, the one that is offered is among the easiest to use and has been shown to be reliable.

The minimum design vapor velocity is given by,

$$\frac{v}{u_\lambda} = \frac{[K_2 - 0.90(25.4 - d_h)]}{(P_v)^{\frac{1}{2}}} \tag{51}$$

where

$\frac{v}{u_\lambda}$ = minimum vapour velocity through the holes (based on the whole area) m/s d_h = hole diameter, mm.

K_2 = a constant, dependent on the depth of clear liquid on the plate, obtained from Figure 16 below.

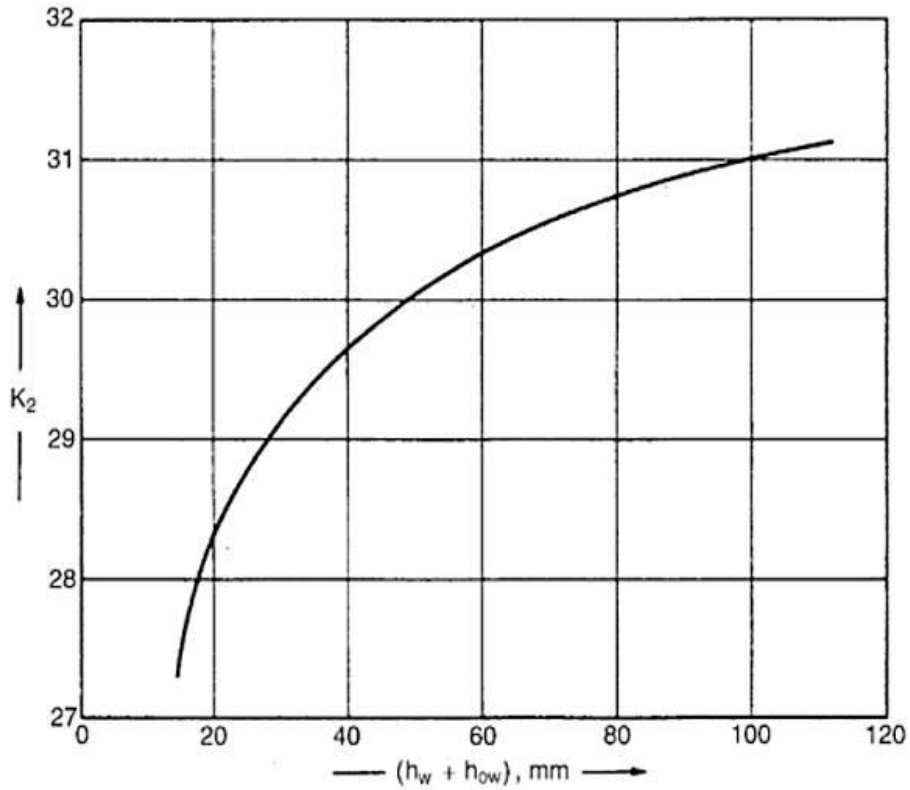

Figure 16. Weeping point correlation [11].

Weir Liquid Crest

The height of the liquid crest over the weir can be estimated using the Francis weir formula. For a segmental downcomer, this can be written as:

$$h_{ow} = 750\left[\frac{L_w}{\rho_L l_w}\right]^{\frac{2}{3}} (52)$$

where, h_{ow} = weir crest, mm liquid, L_w = liquid flow rate, kg/s. and l_w = weir length, m.

The column wall restricts liquid flow in segmental downcomers, causing the weir crest to be higher than that predicted by the Francis formula for flow over an open weir. To account for this result, the constant in Equation (52) has been increased. The crest should be at least 10 mm at the lowest liquid rate to provide a uniform flow of liquid along the weir. Sometimes, very low liquid rates require the use of serrated weirs.

Weir Dimension

Weir Height

The volume of liquid on the plate is determined by the weir's height, which also plays a significant role in determining the effectiveness of the plate. The effectiveness of the plates will rise with a high weir, but at the expense of a greater plate pressure drop. Weir heights for columns operating above atmospheric pressure will typically range from 40 mm to 90 mm (1.5 to 3.5 in.); 40 to 50 mm is advised. Lower weir heights are utilized in vacuum operations to lessen the pressure drop; 6 to 12mm (1/4 to 12 in.) is recommended.

Inlet Weirs

Inlet weirs or recessed pans can occasionally be used with segmental downcomers to improve the distribution of liquid throughout the plate.

Weir Length

In the case of segmental downcomers, the length of the weir fixes the downcomer's area. The chord length will typically range from 0.6 to 0.85 times the diameter of the column. The starting value of 0.77, or a downcomer area of 12%, is a decent one to employ. Figure 17 shows the correlation between weir length and downcomer area. The width of the central downcomer for double-pass plates is typically 200 to 250 mm (8–10 in.).

Perforated $A = \pi r^2$

The restrictions imposed by structural members (such as support rings and beams) and the use of calming zones will both reduce the space that can be perforated.

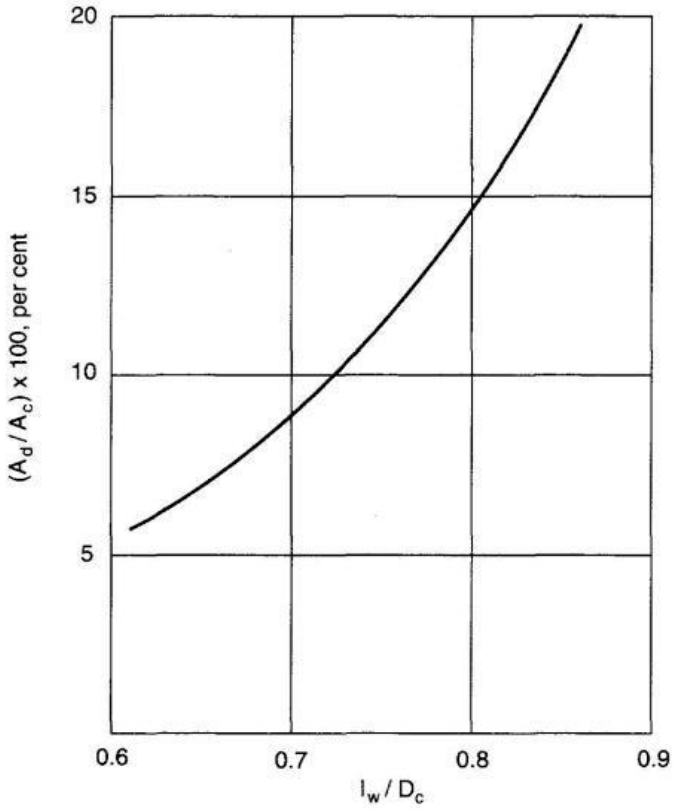

Figure 17. Relationship between downcomer area and weir length.

The unperforated portions of the plate at the inlet and exit sides are referred to as "calming zones." For each zone, the recommended width is 75 mm for areas smaller than 1.5 m in diameter and 100 mm for areas larger than this. For sectional plates, the support ring should normally be 50 to 75 mm broad and should not extend into the downcomer area. To reinforce the plate, a strip of unperforated plate is left around the border of cartridge-style trays. The unperforated area can be calculated using the plate geometry. The relationship between the weir chord's height, length, and angle subtended by the chord is depicted in Figure 18.

Size of the Hole

The ideal hole size is 5 mm; however, the typical range is 2.5 to 12 mm. larger holes are occasionally used for fouling systems. Either drilling or punching is used to create the holes. Punching is less expensive, but the thickness of the plate determines the smallest hole that may be created. Carbon steel can have holes punched that are about the same thickness as the plate, whereas stainless steel can only have holes that are about twice as thick. The standard plate thicknesses for stainless steel and carbon steel are 3 mm (12 gauge) and 5 mm (3/16 in.), respectively.

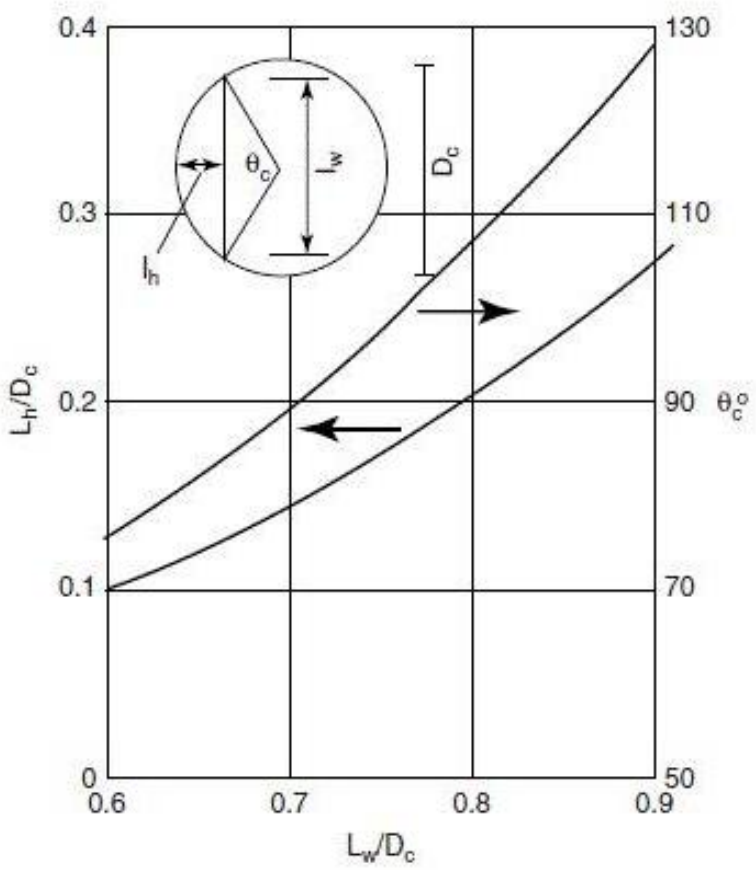

Figure 18. Relationship between the weir chord length, chord height and the angle subtended.

Hole Pitch

The hole pitch (the separation between the centers of the holes) should be at least 2.0-hole diameters, with a typical range of 2.5 to 4.0 diameters. Within this range, the pitch can be chosen to provide the necessary number of active holes for the stated total hole area.

Before deriving the value of l_p/d_h from Figure 19, it is necessary to establish the ratio of the area of the hole to the area of perforation (A_h/A_p), which determines the hole pitch (lp). Total Area of perforation A_p is obtained by geometry.

A_p = Active Area – Area of unperforated Edge – Area of calming zone

$$= A_a - A_{up} - A_{cz} \quad (54)$$

Area of unperforated edge (A_{up}) = Mean Length of unperforated strip × Width of perforated plate = $L_{up} \times W_{up}$ (W_{up} = 50 mm)

But Mean Length of unperforated strip,

$$L_{up} = (D_c - W_{up})\pi \times (180 - \theta c)/180 \quad (55)$$

where, θc is obtained from Figure 19, by first calculating L_w/D_c, hence from Figure 19 ($\pi = 22/7$).

$$\text{Angle subtended by the edge of plate} = 180 - \theta c \quad (56)$$

$$\text{Area of calming zone} = 2(L_{cz} \times W_{cz}) \quad (57)$$

Mean length of calming zone,

L_{cz} = weir length + width of unperforated strip (58)

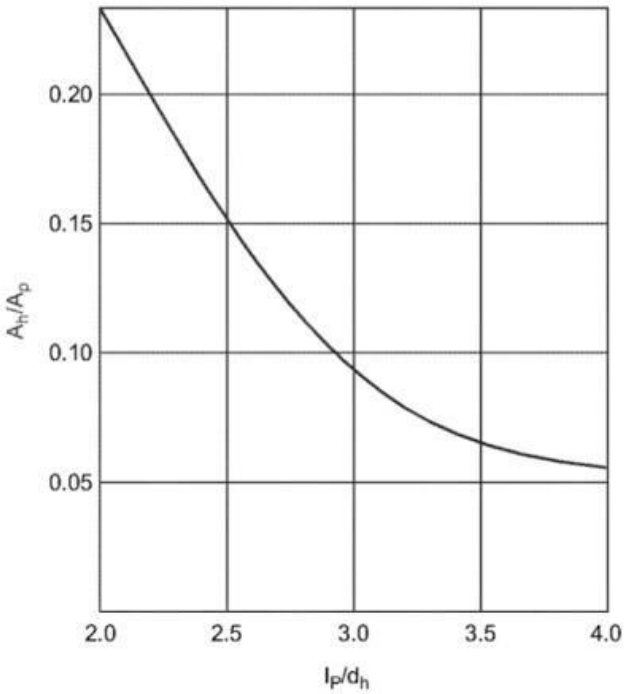

Figure 19. Relationship between hole area and pitch.

Liquid Throw

The horizontal distance covered by the liquid stream as it crosses the downcomer weir is known as the liquid throw. Only in the design of multiple-pass plates is it a crucial factor. A method for calculating the liquid throw is provided.

Drop in Plate Pressure

The pressure drops over the plates is a crucial design consideration. The flow of vapor through the holes (an orifice loss) and the static head of liquid on the plate are the two primary causes of pressure loss. A simple additive model is frequently used to anticipate the total pressure loss. The total is calculated by adding the head of clear liquid on the plate (hw + how), the pressure drop anticipated for the flow of vapor through the dry plate (the dry plate drops hd), and a term to account for other, minor loss (the so-called residual loss hr).

Figure 20 shows the difference between the observed experimental pressure drop and the residual loss obtained by simply adding the clear-liquid height and the dry-plate drop. It considers the energy needed to produce the vapor bubbles as well as the fact that the liquid head on an operating plate will be a head of "aerated" liquid froth, which will have a different density and height than the clear liquid. It is feasible to use liquid millimeters to represent pressure drops. In pressure units, this is how the total pressure drop is computed.

$$h_t = h_d + (h_w + h_{ow}) + h_r \quad (59)$$

$$\Delta P_1 = 9.81 \times 10^{-3} h_l \rho_L \quad (60)$$

where ΔP_1 = total plate pressure drops, Pa(N/m^2) and h_l = total plate pressure drops, mm liquid.

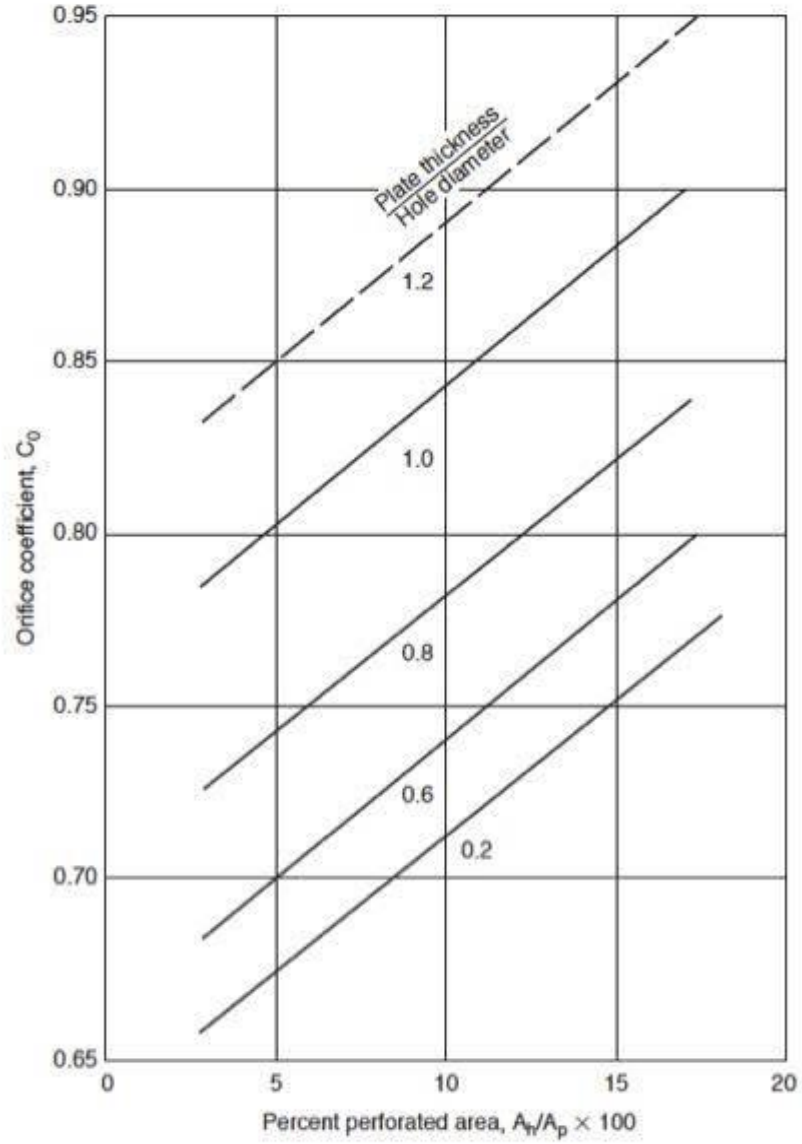

Figure 20. Discharge coefficient sieve plate.

Residual Head Techniques have been proposed to determine the residual head as a function of the liquid's surface tension, froth density, and froth height. Since this correction term is small and the requirement for a complex calculation process is not warranted, the simple equation that has been proposed can be used in its place.

$$h_r = \frac{12.5\times10^3}{\rho_L} \tag{61}$$

Equation (61) is equivalent to taking the residual drop as a fixed value of 12.5 mm of water.

Total Pressure Drop

The total plate drop is given by,

$$h_t = h_d + (h_w + h_{ow}) + h_r \tag{62}$$

If the hydraulic gradient is significant, half of its value is added to the clear liquid height.
Pressure drops through the dry plate,

$$h_d = 51\left[\frac{U_h}{C_o}\right]^2 \frac{\rho_v}{\rho_L} \quad (63)$$

Design of Downcomers

The downcomer area and plate spacing need to be planned so that the liquid and froth level in the downcomer is much lower than the output weir top on the plate above. If the level climbs above the outflow weir, the column will flood. The liquid backs up in the downcomer due to the downcomer's intrinsic flow resistance and the pressure drop over the plate (the downcomer essentially forms one leg of a U-tube).

The following provides the downcomer backup for clear liquid,

$$h_b = (h_w + h_{ow}) + h_{dc} + h_t \quad (64)$$

where h_b = downcomer back-up, measured from the surface mm, h_{dc} = head loss in the downcomer, mm.

The constriction at the downcomer outlet will be the primary source of flow resistance, and the head loss in the downcomer can be calculated using the equation stated below as well as using Figure 21.

$$h_{dc} = 166\left[\frac{L_{wd}}{\rho_L A_m}\right] \quad (65)$$

where L_{wd} = liquid flow rate in downcomer, kg/s and A_m = either the downcomer area A_d or the clearance area under the downcomer A_{ap}; whichever is the smaller, m^2.
The clearance area under the downcomer is given by,

$$A_{ap} = h_{ap} l_w \quad (66)$$

where, h_{ap} is height of the bottom edge of the apron above the plate. This height is normally set 5 to 10mm $\left(\frac{1}{4}\right| \quad \left|\frac{1}{2} \in.\right)$ below the outlet weir height.

$$H_{ap} = h_w - (5 \text{ to } 10 \text{ mm}) \quad (67)$$

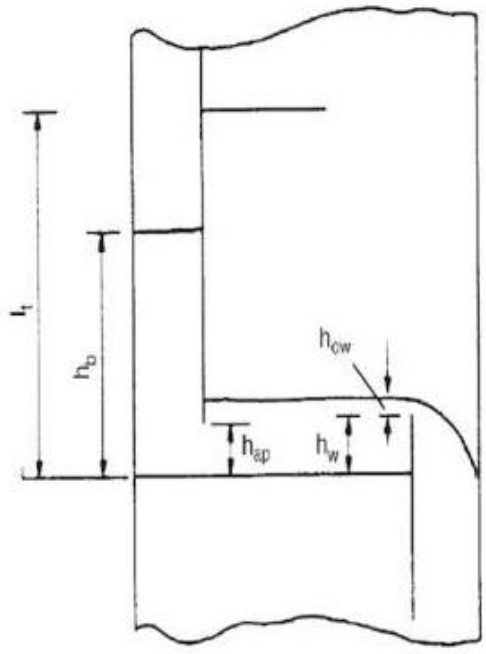

Figure 21. Downcomer backup.

Height of Froth

To forecast the height of "aerated" liquid on the plate and the height of froth in the downcomer, a technique for estimating the froth density is necessary. The density of the "aerated" liquid is usually 0.4 to 0.7 times higher than that of the clear liquid. Since no correlation is very trustworthy, an average value of 0.5 of the liquid density is usually appropriate for design purposes. For predicting the froth density as a function of the liquid's physical characteristics and the vapor flow rate, several correlations have been put out. None is very trustworthy, though numerous connections have been put forth to estimate the froth density in relation to the physical characteristics of the liquid and the vapor flow rate. None, nevertheless, is very trustworthy. The clear liquid backup should be estimated for safety and should not exceed half the plate spacing it to prevent flooding. This value is also considered the mean density of the fluid in the downcomer.

Allowing for the weir height,

$$h_b < \frac{1}{2}(l_t + h_w) \tag{68}$$

Downcomer Residence Time

Sufficient residence time must be allowed in the downcomer for the entrained vapor to disengage from the liquid stream, to prevent heavily "aerated" liquid being carried under the downcomer. A time of at least 3 seconds is recommended.

The downcomer residence time is given by,

$$t_r = \frac{A_d h_{bc} \rho_L}{L_{wd}} \tag{69}$$

where $t_r =$ residence time, s, and $h_{bc} =$ clear liquid back-up, m.

RESULTS AND DISCUSSION

The design data parameter to achieve the aim and object of the research are presented in Table 1 below. Other information can be obtained from the various charts presented in the research.

Table 1. Design data for various packings [4].

	Size		Bulk density (kg/m^3)	Surface area a (m^2/m^3)	Packing factor $F_p m^{-1}$
	in.	mm			
Raschig rings ceramic	0.50	13	881	368	2100
	1.0	25	673	190	525
	1.5	38	689	128	310
	2.0	51	651	95	210
	3.0	76	561	69	120
Metal (density for carbon steel)	0.5	13	1201	417	980
	1.0	25	625	207	375
	1.5	38	785	141	270
	2.0	51	593	102	190
	3.0	76	400	72	105
Pall rings	0.625	16	593	341	230
metal	1.0	25	481	210	160
(density for carbon steel)	1.25	32	385	128	92
	2.0	51	353	102	66
	3.5	76	273	66	52
Plastics	0.625	16	112	341	320
(density for polypropylene)	1.0	25	88	207	170
	1.5	38	76	128	130
	2.0	51	68	102	82
	3.5	89	64	85	52
Intalox saddles	0.5	13	737	480	660
ceramic	1.0	25	673	253	300
	1.5	38	625	194	170
	2.0	51	609	108	130
	3.0	76	577		72

The following conceptual applications were needed to achieve effectiveness in the design of CO_2 capture from amine plants as demonstrated below,

1. The process flow diagram for CO_2 absorption.
2. Schematic diagram of post combustion capture.
3. Process flow diagram for CO_2 capture.
4. Schematic diagram of a packed bed absorption column undergoing countercurrent operation.
5. Generalized pressure drop correlation for K_4.
6. Gas absorption concentration relationship.
7. Number of overall gas phase mass transfer units in a packed column.
8. Chart of flooding calculation.
9. Distillation column (a) basic column (b) multiple feed.
10. Column flow and composition above and below feed.
11. Different types of q-line.
12. McCabe–Thiele plot.
13. Flooding velocity sieve plate, selection of liquid flow arrangement.
14. Entrainment correlations of sieve plates.
15. Weeping point correlation.
16. Relationship between downcomer area and weir length.
17. Relationship between weir chord length.
18. Chord height and the angle subtended.
19. Relationship between hole area and pitch.
20. Discharge coefficient sieve plate.
21. Downcomer back up.

CONCLUSIONS

The following conclusions were outlined from the research as stated below.

1. This research shows that carbon dioxide can be captured in the environment to avoid unforeseen circumstances.
2. Optimization of the process should be considered in future work to maximize the yield of carbon capture.
3. The world population cannot easily stop the production of fossil fuels to meet energy demands of the country which implies that carbon dioxide can be utilized.
   CO_2 must be recovered from fossil fuel and be utilized with hydrogen to produce methane which can also be used as fuel.

REFERENCES

1. Ogoni HA, Ukpaka CP. Instrumentation, process control and dynamics. 1st ed. Washington, DC: Library of Congress Cataloging in Publication Data; 2004. p. 153–86.
2. Crooks JE, Donnellan JP. Kinetics and mechanism of the reaction between carbon dioxide and amines in aqueous solution. J Chem Soc Perkin Trans 2. 1989;(4):331–3.
3. Davison J, Bressan L, Domenichini R. Carbon dioxides capture in coal-based IGCC power plants. In: Proceedings of the 7th International Conference on Greenhouse Gas Control Technologies. Vancouver, Canada; 2004.
4. Diao YF, Zheng XY, He BS, Chen CH, Xu XC. Experimental study on capturing CO_2 greenhouse gas by ammonia scrubbing. Energy Convers Manag. 2004;45:2283–96.
5. Dugas RE. Pilot plant study of carbon dioxide capture by aqueous monoethanolamine [master's thesis]. Austin (TX): The University of Texas at Austin; 2006.
6. Geankoplis CJ. Transport processes and separation process principles. 4th ed. Upper Saddle River (NJ): Prentice Hall; 2003. p. 686.
7. Kanniche M, Gros-Bonnivard R, Jaud P, Valle-Marcos J, Amann J-M, Bouallou C. Pre-combustion, post-combustion and oxy-combustion in thermal power plant for CO_2 capture. Appl Therm Eng. 2010;30:53–62.
8. Khaisri S, DeMontigny D, Tontiwachwuthikul P, Jiraratananon R. CO_2 stripping from monoethanolamine using a membrane contactor. J Membr Sci. 2011;376:110–8.

9. Eliasson B, Riemer P, Wokaun A, editors. R&D options. In: Greenhouse Gas Control Technologies. Proc 4th Int Conf Greenhouse Gas Control Technologies. Interlaken, Switzerland. Oxford: Elsevier Science Ltd.; 1998 Aug 30–Sep 2. p. 119–24.
10. Reddy S, Scherffius J, Freguia S, Fluor RC. Econamine TM FG PlusSM technology: An enhanced amine-based CO_2 capture process. In: Proceedings of the 2nd National Conference on Carbon Sequestration. Alexandria, VA; 2003.
11. Richardson JF, Harker JH. Coulson and Richardson's chemical engineering: Particle technology and separation processes. 5th ed. Oxford (UK): Butterworth-Heinemann; 2002.
12. Singh D, Croiset E, Douglas PL, Douglas MA. Techno-economic study of CO_2 capture from an existing coal-fired power plant: MEA scrubbing vs. O_2/CO_2 recycle combustion. Energy Convers Manag. 2003;44:3073–91.
13. Ukpaka CP, Ogoni HA, Amadi SA, Njobuenwu DO. Mathematical modelling of the fluid screw positive displacement pump using pump scaling laws method. Int J Sci Technol. 2005;4(2):16–22.
14. Ukpaka CP. Modeling solid–liquid separation on a rotating vertical cylinder. Multidiscip J Empir Res. 2005;2(2):53–63.
15. Ukpaka CP, Ogoni HA, Ikenyiri PN. Development of mathematical models for the rheological test, velocity distribution and flow rate characteristic of crude oil flowing through a tube of various radii. J Model Simul Control AMSE. 2005;74(8):23–42.
16. Ukpaka CP. Modeling solid–gas separation in a cyclone operating system. J Sci Ind Stud. 2007;5(1):39–45.

